Available online at www.sciencedirect.com
SCIENCE DIRECT®
ELSEVIER
Nuclear Instruments and Methods in Physics Research B 241 (2005) 43–47
NIM B
Beam Interactions with Materials & Atoms
www.elsevier.com/locate/nimb

On the effect of image states on resonant neutralization of hydrogen anions near metal surfaces

Himadri S. Chakraborty *, Thomas Niederhausen, Uwe Thumm *

James R. Macdonald Laboratory, Department of Physics, Kansas State University, Manhattan, KS 66506-2604, USA

Available online 25 August 2005

Abstract

We directly assess the role of image state electronic structures on the ion-survival by comparing the resonant charge transfer dynamics of hydrogen anions near Pd(1 1 1), Pd(1 0 0), and Ag(1 1 1) surfaces. Our simulations show that image states that are degenerate with the metal conduction band favor the recapture of electrons by outgoing ions. In sharp contrast, localized image states that occur inside the band gap hinder the recapture process and thus enhance the ion-neutralization probability.
© 2005 Elsevier B.V. All rights reserved.

PACS: 79.20.Rf; 34.70.+e; 73.20.At

Keywords: Image state; Surface; Charge transfer

1. Introduction

Charge-transfer in ion-surface collisions is a fundamental process in several branches of applied physics and chemistry, such as, plasma–wall interactions in ion-sources, reactive ion-etching, and secondary ion mass spectroscopy [1,2]. It is also of basic research interest, since the electronic dynamics that eventually determines the final charge state of a reflected ion depends sensitively on the electronic structure of the target surface [3,4]. Affinity levels of atomic anions are energetically above and clearly separated from the Fermi level of most FCC-metal surfaces. For such systems, the dominant neutralization mechanism is resonant charge transfer (RCT) [4–11]. Due to its simplicity, this one-electron process is particularly attractive for theoretical investigations.

For H^- scattering off Cu(1 1 1), detailed calculations on the effect of projected L-band gap and a Shockley surface state on the RCT process were performed [7]. More recently, the influence of

* Corresponding authors. Tel.: +1 225 578 0554; fax: +1 225 578 5855 (H.S. Chakraborty), tel.: +1 785 532 1613; fax: +1 785 532 6806 (U. Thumm).
E-mail addresses: himadri@phys.ksu.edu (H.S. Chakraborty), thumm@phys.ksu.edu (U. Thumm).

0168-583X/$ - see front matter © 2005 Elsevier B.V. All rights reserved.
doi:10.1016/j.nimb.2005.07.185

crystallographic surface symmetry on RCT, i.e. the effect of altering energetic positions of band gaps, surface states, and image states, has been investigated for Ag [8] and Cu [9] surfaces. These single-electron calculations are in fair agreement with measurements [8]. However, apart from some qualitative insight [9], the effects of image states on RCT has not been assessed quantitatively. We address this issue here by comparing the neutralization dynamics of H^- in front of Pd and Ag(111) surfaces. Pd(111) and Pd(100) are ideal candidates for this study, because (i) image states for both surfaces are localized, (ii) the Fermi energy (E_F) of either surface being far below the conduction band (Fig. 1) makes many-body quantum statistical effects irrelevant, and (iii) the surfaces are experimentally amenable [11].

In the following section we briefly outline our theoretical methodology. Our numerical results are discussed in Section 3. The final section contains our conclusions. Unless stated otherwise, we use atomic units.

2. Theory

The time-dependent electronic wave function $\Phi(\boldsymbol{r}, t, D)$ for the ion-surface system is a solution of the time-dependent Schrödinger equation with the Hamiltonian

$$H = -\frac{1}{2}\frac{d^2}{dz^2} - \frac{1}{2}\frac{d^2}{dx^2} + V_{\text{ion}} + V_{\text{surface}}, \tag{1}$$

where V_{ion} and V_{surface} are effective potentials for the ion and the surface, and D denotes the ion-surface distance. Considering the asymptotic initial wave function $\Phi(\boldsymbol{r}, t = 0; D = \infty)$ to be the unperturbed H^- wave function, $\varphi_{\text{ion}}(\boldsymbol{r})$, that is bound by V_{ion}, the propagation of $\Phi(\boldsymbol{r}, t, D(t))$ by one time step Δt yields

$$\Phi(\boldsymbol{r}, t + \Delta t, D) = \exp[-iH(D)\,\Delta t]\Phi(\boldsymbol{r}, t, D). \tag{2}$$

The ion-survival amplitude (or autocorrelation), is then given by the overlap

$$A(t) = \langle \Phi(\boldsymbol{r}, t, D) | \varphi_{\text{ion}}(\boldsymbol{r}) \rangle. \tag{3}$$

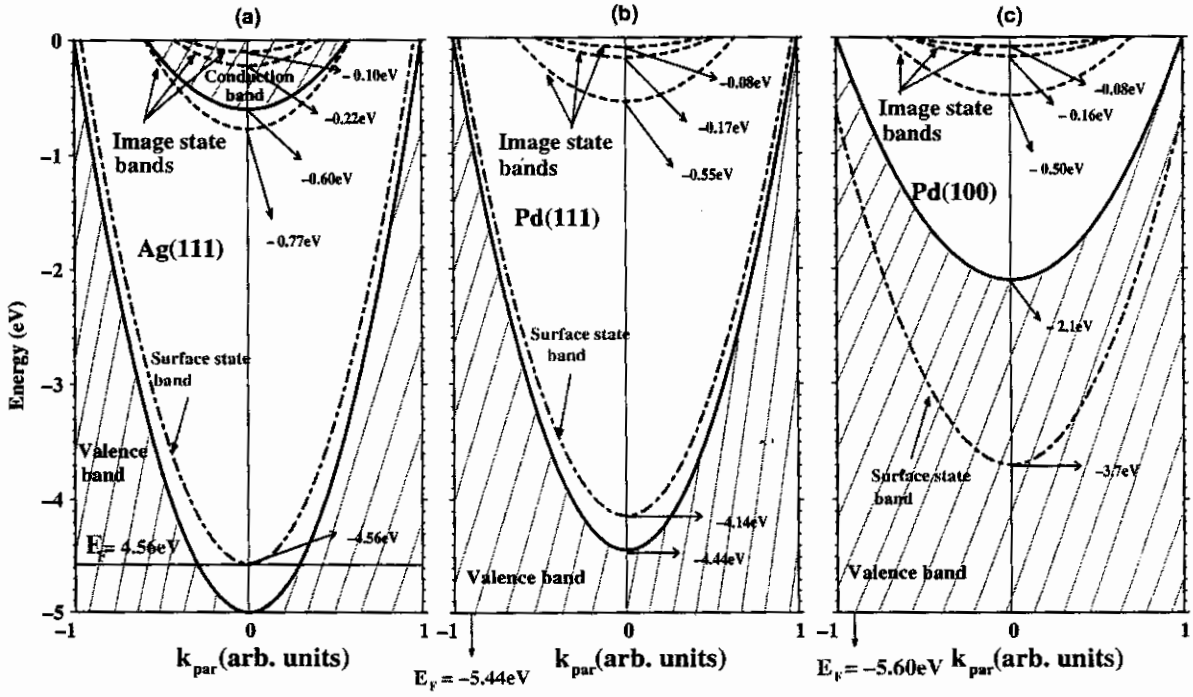

Fig. 1. Schematic of the electronic structure of Ag(111), Pd(111) and Pd(100) surfaces. For free electron motions on the surface plane, dispersions corresponding to the band gaps, the surface states, and the image states are shown. The Fermi energy (E_F) for each surface is indicated. The bottoms of the conduction band for Pd(111) and Pd(100) are at 2.16 eV and 5.0 eV, respectively.

We employ the split-operator Crank–Nicholson propagation method (CNP) in conjunction with the unitary and unconditionally stable Cayley scheme to evaluate $\Phi(r,t,D)$ after successive time steps [8,9,12]. In order to keep the computing time at a manageable level, we employ a 2-d numerical grid which limits the electronic dynamics to the scattering plane. Our x and z axis are oriented in directions parallel and normal to surface, and the surface is assumed to be translationally invariant along the x direction.

During the (assumed) specular reflection, the incident ion decelerates along the z direction, close to the surface, due to the net repulsive interaction between the ion-core and surface atoms. For a given initial kinetic energy E and angle of incidence (=angle of exit) Θ of the ion with respect to the surface normal, we simulate a classical trajectory based on "Biersack–Ziegler" interatomic potentials [13,9]. Long after the surface reflection, the final ionic survival probability is obtained by

$$P_{2\text{-d}}(E,\Theta) = \lim_{t\to\infty} |A(t)|^2, \tag{4}$$

where the subscript refers to the reduced-dimensionality of our calculation. Assuming equal transition rates of the projectile electron along both surface direction (x and y direction), we approximate the ion-survival probability in full (3-d) dimensionality as [8]

$$P_{3\text{-d}}(E,\Theta) \approx [P_{2\text{-d}}(E,\Theta)]^2. \tag{5}$$

The H^- ion is described by an effective single-electron model potential, V_{ion}, that includes the interaction of a polarizable hydrogen core with the active electron [14]. To be consistent with our 2-d wave-packet propagation scheme, we modify the model ion-potential appropriately [8,9], ensuring the correct electron affinity of 0.76 eV. The surface potentials, V_{surface}, are constructed by the z-dependent single-electron potentials that are modeled on the basis of pseudopotential local density approximation calculations [9,15].

3. Results and discussion

Energy dispersion curves for the Ag(1 1 1), Pd(1 1 1) and Pd(1 0 0) surfaces along the surface normal are schematically presented in Fig. 1. The energies of various states supported by the 1-d surface potential, V_{surface}, are given at free momenta parallel to the surface $k_{\text{par}} = 0$. Comparing Fig. 1(a) with (b), the electronic structures of Ag(1 1 1) and Pd(1 1 1) show one main difference. Except for the first image state all higher image states are degenerate with the conduction band of Ag(1 1 1), whereas the whole Rydberg series of Pd(1 1 1) image states lie well inside the band gap and, therefore, are localized along the surface normal. Comparing Pd(1 1 1) and Pd(1 0 0) (Fig. 1(b) and (c)) we note that both surfaces have similar image state structures, but surface states are of very different character: the Pd(1 1 1) surface state appears in the band gap while that for Pd(1 0 0) is embedded in the valence-band. We therefore expect the comparison between measurable ion survival probabilities after the scattering off these surfaces to directly reveal effects due of these distinct differences in surface electronic structures.

This is shown in Fig. 2, where the percentage survival probabilities (5) for 1 keV H^- ions scattered from Ag(1 1 1) and the two Pd surfaces are presented as a function of Θ. Except for nearly normal incidence ($\Theta \sim 90°$), our results for $P_{3\text{-d}}(E,\Theta)$ are significantly larger for Ag(1 1 1) than Pd(1 1 1) for most angles of incidence. This is due

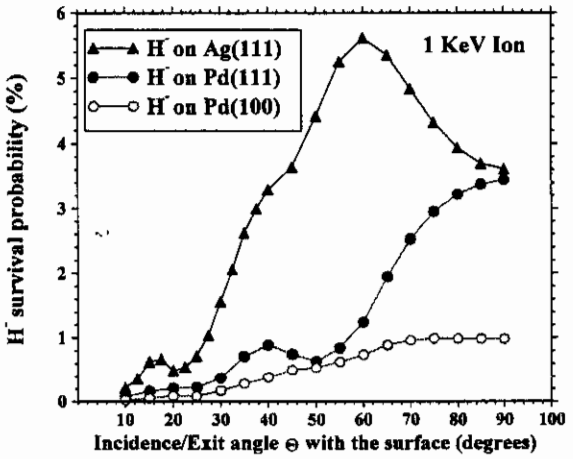

Fig. 2. Percentage survival probability of 1 keV H^- ions scattered from Ag(1 0 0), Ag(1 1 1) and Pd(1 0 0) surfaces as a function of the incident angle (=exit angle) with respect to the surface plane.

to the different character of Ag(1 1 1) and Pd(1 1 1) image states. As already pointed out and shown in Fig. 1(a) and (b), in contrast to the localized Pd(1 1 1) image states, Ag(1 1 1) image states are coupled to the bulk conduction band. Therefore, while populated image states near Pd(1 1 1) evolve away from the surface region towards the vacuum, electrons in the Ag(1 1 1) image states return towards the bulk and re-populate the surface region. As a consequence, the outgoing depleted projectile has a larger probability for electron recapture near the Ag(1 1 1) surface, due to its wave function overlap with occupied substrate states near the surface region.

The surface states of both (1 1 1) surfaces being similar in character (Fig. 1(a) and (b)) are not expected to contribute to the large differences in the ion-survival probabilities. Of course, the stronger ion-neutralization for the Pd(1 0 0) compared to Ag(1 1 1) surface in Fig. 2, in particular for steep incidences, also owes to differences between their surface states [8,9]. The Pd(1 0 0) surface state is embedded in the valence-band and readily decays into the bulk, in contrast to the less efficient decay of the localized Ag(1 1 1) surface state. This further reduces the electron probability density at the Pd(1 0 0) surface and suppresses recapture by the ion for Θ above 60°. A more direct assessment of this surface state effect is evident by comparing results of Pd(1 1 1) with Pd(1 0 0). Below $\Theta = 60°$, however, the close predictions for Pd(1 1 1) and Pd(1 0 0), plus their similar differences from Ag(1 1 1) results, indicate a predominant influence of the image state dynamics in the neutralization process.

To further illustrate the main effect, we distinguish two regions of the ion-surface interaction. In region I, the incoming trajectory populates first the surface state and, at closer distances, the image states. In region II, the reflected and depleted ion recaptures electrons from the surface. These two regions are shown in Fig. 3, where for 50° incidence $|A(t)|^4$ is plotted against the distance of the ion from its position of closest approach. For all three surfaces, the effective electron loss on the incoming trajectory are similar. Clearly, the final ion-survival most sensitively depends on electron recapture on the outgoing trajectory. There, in region II, similar ion-survivals near the Pd surfaces and the large difference between Pd and Ag(1 1 1) results emphasize the overwhelming role of image states in determining the final projectile charge state.

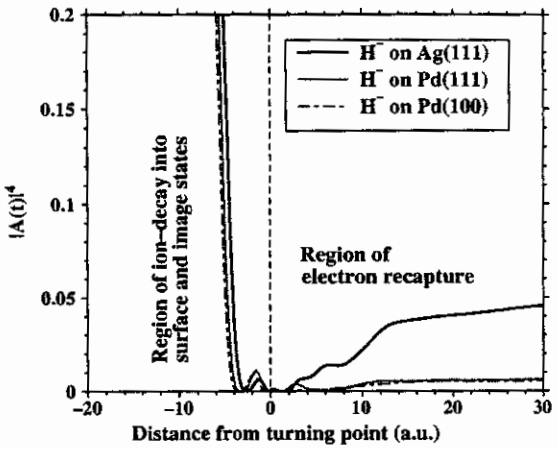

Fig. 3. $|A(t)|^4$ as a function of the vertical distance from the turning point for incident 1 keV H^- ions. Negative and positive distances are for the incoming and outgoing segment of the trajectory, respectively. The angle of incidence with respect to the surface is 50°. Two distinct interaction regions are indicated.

Fig. 4 visualizes the image state dynamics in terms of snapshots of the probability density $|\Phi(r,t,D)|^2$ for Ag(1 1 1) and Pd(1 1 1) targets at a time of 50 a.u. after the projectile has reached the position of closest approach to the surface. The ion was incident from below the straight line representing the surface. The population of the Schockley surface state for both surfaces and their similar decay along the parallel direction is seen. However, the main difference in the electron density emerges at large distances on the vacuum side. For Ag(1 1 1) the populated image states are seen to more readily decay into the bulk through their coupling with the conduction band. On the other hand, for Pd(1 1 1) a bulging bigger hemisphere, representing the populated localized image states, is pushing the electronic density away from the surface. The larger electron probability current density into the Ag(1 1 1) bulk is clearly seen; so is the larger density distribution near the projectile nucleus that indicates a higher rate of electron-recapture near the Ag(1 1 1) surface.

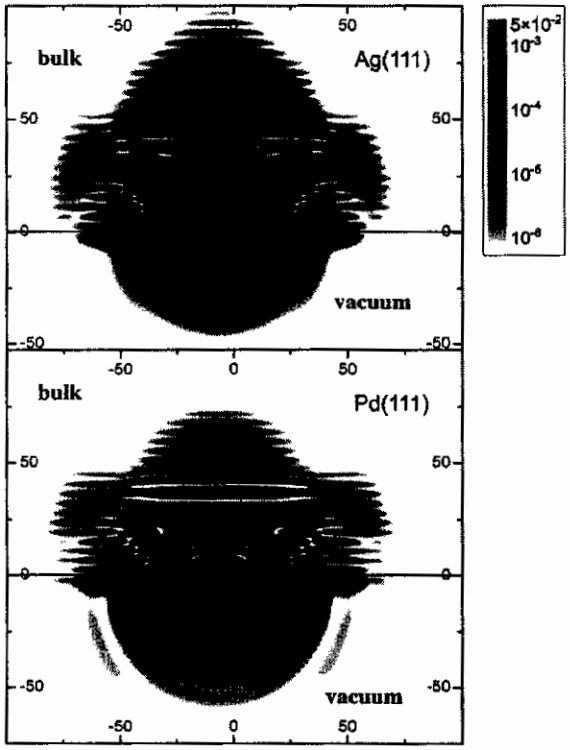

Fig. 4. Electronic probability (logarithmic scale) for Ag(1 1 1) (upper panel) and Pd(1 1 1) surfaces at a time of 50 a.u. after the projectile has reached the position of closest approach to the surface. The ion approaches the surface at an angle of 50° with respect to the surface and with an energy of 1 keV. The region below the straight line, indicating the surface, is the vacuum region.

4. Conclusion

We have shown that different H^- neutralization probabilities near Ag(1 1 1) and Pd(1 1 1) surfaces are mainly due to dissimilar characters of their respective image states. The conduction-band-embedded image states in Ag(1 1 1) strongly favor electron recapture, while localized image states in Pd(1 1 1) drive the electrons away from the ion and hinder recapture. By comparing these results with the results for Pd(1 0 0), we found that the effect of the Schockley surface state in Pd(1 1 1) can only counter this image state effect over a small range of incidence angles near the normal incidence.

Acknowledgments

This work was supported by the NSF (Grant PHY 0071035) and the Division of Chemical Sciences, Office of Basic Energy Sciences, Office of Energy Research, US DOE.

References

[1] J.P. Gauyacq, A. Borisov, D. Teillet-Billy, in: V. Esaulov (Ed.), Formation/Destruction of Negative Ions in Heavy Particle-Surface Collisions, Cambridge University Press, 1996.
[2] H. Shao, D.C. Langreth, P. Nordlander, in: J.W. Rabalais (Ed.), Low Energy Ion-Surface Interactions, Wiley, New York, 1994, p. 118.
[3] S. Wethekam, A. Mertens, H. Winter, Phys. Rev. Lett. 90 (2003) 037602.
[4] Y. Yang, J.A. Yarmoff, Phys. Rev. Lett. 89 (2002) 196102.
[5] L. Guillemot, V.A. Esaulov, Phys. Rev. Lett. 82 (1999) 4552.
[6] T. Hecht, H. Winter, A.G. Borisov, J.P. Gauyacq, A.K. Kazansky, Phys. Rev. Lett. 84 (2000) 2517.
[7] A.G. Borisov, A.K. Kazansky, J.P. Gauyacq, Phys. Rev. B 59 (1999) 10935.
[8] H.S. Chakraborty, T. Niederhausen, U. Thumm, Phys. Rev. A 69 (2004) 052901.
[9] H.S. Chakraborty, T. Niederhausen, U. Thumm, Phys. Rev. A 70 (2004) 052903.
[10] A.G. Borisov, A. Mertens, S. Wethekam, H. Winter, Phys. Rev. A 68 (2003) 012901.
[11] E. Sanchez, L. Guillemot, V.A. Esaulov, Phys. Rev. Lett. 83 (1999) 428.
[12] W.H. Press, S.A. Teukolsky, W.T. Vellerling, B.P. Flannery, Numerical Recipes in FORTRAN, Cambridge University Press, Cambridge, 1993.
[13] J.P. Biersack, J.F. Ziegler, Nucl. Instr. and Meth. B 194 (1982) 93.
[14] V.A. Ermoshin, A.K. Kazansky, Phys. Lett. A 218 (1996) 99.
[15] E.V. Chulkov, V.M. Silkin, P.M. Echenique, Surf. Sci. 437 (1999) 330.